Comprehensive structure-activity-relationship of azaindoles as highly potent FLT3 inhibitors

Grimm, S.H.; Gagestein, B.; Keijzer, J.F.; Liu, N.; Wijdeven, R.H.; Lenselink, E.B.; ... ; Stelt, M. van der

Bioorganic & Medicinal Chemistry xxx (xxxx) xxx–xxx

Contents lists available at ScienceDirect

Bioorganic & Medicinal Chemistry

journal homepage: www.elsevier.com/locate/bmc

Comprehensive structure-activity-relationship of azaindoles as highly potent FLT3 inhibitors

Sebastian H. Grimm[a], Berend Gagestein[a], Jordi F. Keijzer[a], Nora Liu[a], Ruud H. Wijdeven[b], Eelke B. Lenselink[c], Adriaan W. Tuin[d], Adrianus M.C.H. van den Nieuwendijk[d], Gerard J.P. van Westen[c], Constant A.A. van Boeckel[e], Herman S. Overkleeft[d], Jacques Neefjes[b], Mario van der Stelt[a,*]

[a] Department of Molecular Physiology, Leiden Institute of Chemistry, Leiden University, Leiden, the Netherlands
[b] Oncode Institute and Department of Cell and Chemical Biology, Leiden University Medical Center, Leiden, the Netherlands
[c] Computational Drug Discovery, Division of Drug Discovery and Safety, Leiden Academic Centre for Drug Research, Leiden University, Leiden, the Netherlands
[d] Department of Bio-Organic Synthesis, Leiden Institute of Chemistry, Leiden University, Leiden, the Netherlands
[e] Pivot Park Screening Center, Oss, the Netherlands

ARTICLE INFO

Keywords:
H-89 analogs
Fms-like tyrosine kinase 3 (FLT3)
Acute myeloid leukemia (AML)
Inhibitors

ABSTRACT

Acute myeloid leukemia (AML) is characterized by fast progression and low survival rates, in which Fms-like tyrosine kinase 3 (FLT3) receptor mutations have been identified as a driver mutation in cancer progression in a subgroup of AML patients. Clinical trials have shown emergence of drug resistant mutants, emphasizing the ongoing need for new chemical matter to enable the treatment of this disease. Here, we present the discovery and topological structure-activity relationship (SAR) study of analogs of isoquinolinesulfonamide H-89, a well-known PKA inhibitor, as FLT3 inhibitors. Surprisingly, we found that the SAR was not consistent with the observed binding mode of H-89 in PKA. Matched molecular pair analysis resulted in the identification of highly active sub-nanomolar azaindoles as novel FLT3-inhibitors. Structure based modelling using the FLT3 crystal structure suggested an alternative, flipped binding orientation of the new inhibitors.

1. Introduction

Acute myeloid leukemia (AML) is a cancer of the blood and bone marrow that is characterized by a failure in differentiation of stem cells during hematopoiesis, resulting in flooding of the bloodstream with immature myeloid blood cells. These blast cells fatally disrupt normal hematopoietic function and their abundance in blood obstruct the normal flow in capillaries resulting in a high mortality.[1,2] While in younger patients cure rates can reach up to 35–40%, elderly patients, who are often unable to cope with the intensive chemotherapy regimen, do not experience this benefit.[3] AML is a genetically diverse disease, but in 20–30% of patients an internal tandem duplication (ITD) in the juxtamembrane domain of the Fms-like tyrosine kinase 3 (FLT3) receptor has been identified as a driver mutation.[4,5] The validation of FLT3 as a drug target led to clinical development of several small molecule inhibitors, culminating in the recent FDA approval of midostaurin for treatment of FLT3-dependent AML in conjunction with standard treatment.[6–9] Although the initial response to treatment with FLT3 inhibitors shows therapeutic promise, many AML patients relapse due to the emergence of drug-resistant cancer cells.[10–12] Resistance-inducing mutations have thus far been observed in treatments with several FLT3 inhibitors, among which the highly potent experimental drug quizartinib.[12–14] The discovery of new chemical entities to target FLT3 represents, therefore, a medical need.

N-[2-(*p*-bromocinnamylamino)ethyl]-5-isoquinolinesulfonamide (H-89) is a prototypical and intensely-studied kinase inhibitor (Figure 1A). It was one of the first non-natural, synthetic inhibitors that competitively inhibited the binding of ATP to the structurally conserved binding domain of cAMP-dependent protein kinase (PKA).[16,17] The binding mode of H-89 to PKA has been studied in great detail at the atomic level using crystallization studies.[18] This contributed to the understanding of kinase function and provided general principles to develop drug-like kinase inhibitors. The isoquinoline sulfonamide mimics the binding mode of adenosine. The nitrogen of the isoquinoline ring forms a crucial H-bond bridge to the backbone of Val-123, located in the hinge region of PKA.[18] This binding mode of H-89 is not specific

* Corresponding author.
E-mail address: m.van.der.stelt@chem.leidenuniv.nl (M. van der Stelt).

https://doi.org/10.1016/j.bmc.2019.01.006
Received 25 November 2018; Received in revised form 8 January 2019; Accepted 10 January 2019

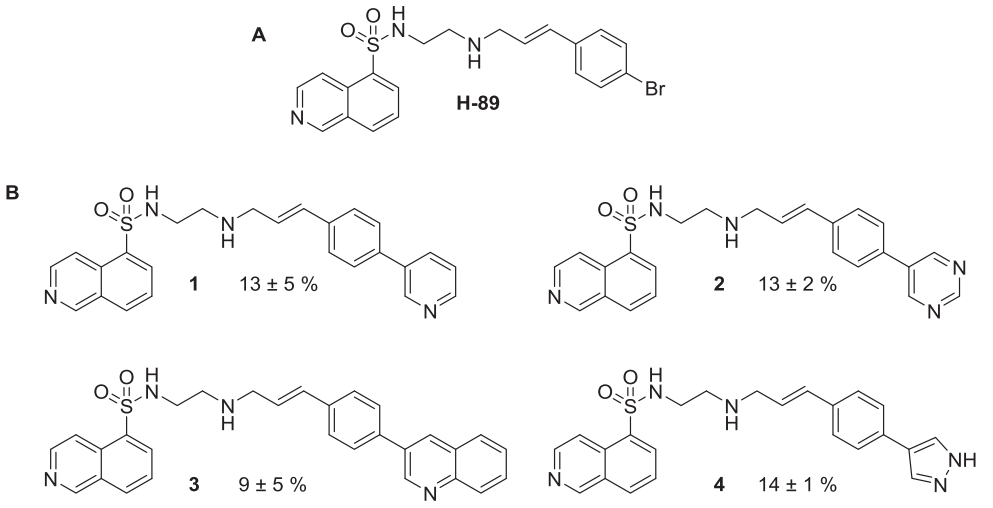

Figure 1. FLT3 screening hits (**1–4**) from an H-89 library.[15] Data represent residual *in vitro* FLT3 activity at 2 μM.

to PKA, but has also been observed with Haspin, as shown in structural data (PDB: 3FMD). Furthermore, H-89 activity has been shown for several other kinases, including S6K1, MSK1 and ROCK-II.[19,20] Consequently, H-89 is used as a starting point in several drug discovery programs. For example, this lab has previously described the use of H-89 and its analogs as RAC-alpha serine/threonine-protein kinase (AKT1) inhibitors to combat bacterial infections, such as *Salmonella typhimurium* and *Mycobacterium tuberculosis*.[15,21] During the hit optimization program of H-89 analogs as AKT1 inhibitors, four compounds (**1–4**) were identified that demonstrated substantial activity against FLT3 (Figure 1B).[15] In this study the optimization and structure-activity relationships of H-89-derived compounds as new FLT3 inhibitors is presented.

2. Results and discussion

To confirm the structure and activity of compound **1**, the synthesis was commenced with the commercially available building blocks as outlined in Scheme 1. After methylation and reduction, the resulting alcohol was exchanged for a chlorine and a trityl protected ethylenediamine linker was introduced via nucleophilic substitution. Subsequent Boc-protection, Suzuki-coupling with 3-pyridinylboronic acid and trityl-deprotection yielded the primary amine, which could be coupled with isoquinoline sulfonyl chloride to provide the desired product **1**. The activity of compound **1** was confirmed in a biochemical assay using purified, recombinantly expressed human FLT3 with a time-resolved fluorescence resonance energy transfer (FRET) method. Compound **1** showed potent inhibition with a half maximum inhibitory concentration (IC_{50}) in the low nanomolar range (pIC_{50} = 8.02 ± 0.05), which was comparable to the inhibitory activity of the reference inhibitor quizartinib (pIC_{50} = 8.30 ± 0.07). Compound **1** demonstrated favorable physico-chemical properties with a molecular weight (MW) of 445 and a logD (pH 7.4) of 1.5.[22] This resulted in a lipophilic efficiency (LipE = pIC_{50} - logD) of 6.5.[23] In summary, compound **1** was defined as an excellent starting point to develop new FLT3 inhibitors.

A topological exploration of the structure-activity relationship of isoquinolinesulfonamides was employed guided by the observed binding mode of H-89 in other kinases.[18] First, the isoquinoline substituent was replaced by various other hinge binding moieties inspired by kinase drugs, including indolones (sunitinib and nintedanib),[24–27] aminoisoquinolines (crizotinib and palbociclib),[24,28,29] indazoles (axitinib)[24,30] and picolinamides (sorafenib).[24,31,32] The analogs (**5–16**) were synthesized in a similar manner as compound **1** using a palladium-catalyzed sulfination of heteroaryl halides and subsequent coupling with the primary amine as shown in Scheme 1.[33] Interestingly, compounds **5–12** displayed similar or slightly weaker activity compared to compound **1** with a range of pIC_{50}s between 7.6 and 8.0 (Table 1). Indazole **6** was the most potent compound of the series with a pIC_{50} of 8.01 ± 0.02.

Moreover, substantially more polar groups such as picolinamide were well tolerated (as observed in compound **10**), resulting in a high

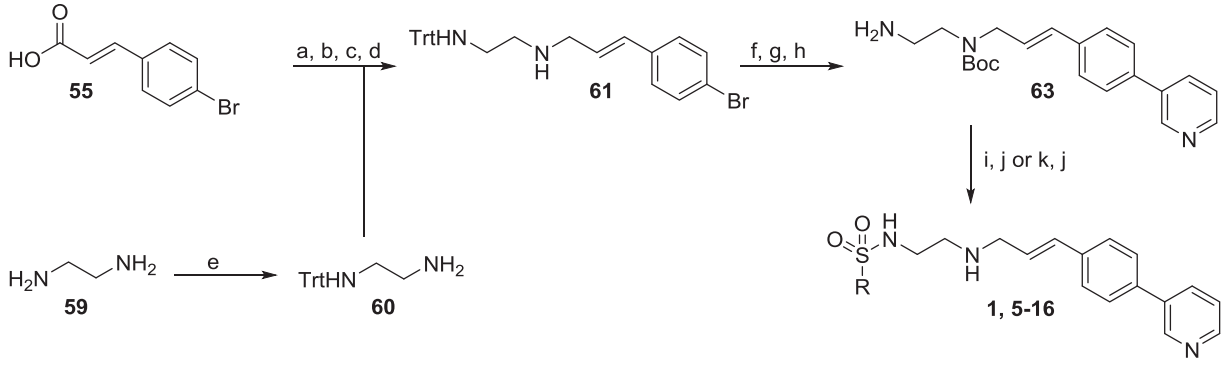

Scheme 1. Synthetic route towards the derivatives **1**, **5–16**.[a]. [a]Reagents and conditions: (a) K_2CO_3, dimethyl sulfate, ACN, 80 °C, overnight; (b) DIBAL-H, toluene, − 80 – 0 °C; (c) $SOCl_2$, DCM, RT; (d) **60**, K_2CO_3, ACN, 70 °C, 2 h; (e) TrtCl, K_2CO_3, RT, 40 min; (f) $NaHCO_3$, Boc_2O, THF, RT, overnight; (g) 3-pyridinylboronic acid, Pd$(PPh_3)_4$, K_2CO_3, DCM/DMF, 85 °C, 6 h; (h) TFA, TES, DCM 0 °C – RT, 5 h; (i) heteroaryl-bromide, $K_2S_2O_5$, HCOONa, $Pd(OAc)_2$, PPh_3, 1,10-phenanthroline, DMSO then DiPEA, **63**, NBS, THF, 0 °C – RT, 1 h; (j) TFA, $CHCl_3$, 1 h; (k) aryl-sulfonylchloride, Et_3N, DCM/DMF, 0 °C – RT.

Table 1
In vitro FLT3 activity and lipophilic efficiency (LipE) of compounds **1 – 18**.

R = 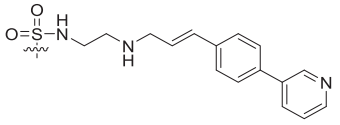

Entry		pIC$_{50}$ ± SEM	LipE	Entry		pIC$_{50}$ ± SEM	LipE
1	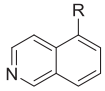	8.02 ± 0.05	6.5	**11**	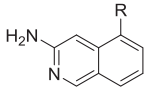	7.71 ± 0.10	6.4
5	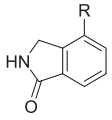	7.70 ± 0.11	7.0	**12**	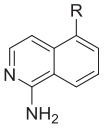	7.62 ± 0.16	6.3
6	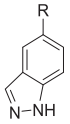	8.01 ± 0.08	6.6	**13**		7.21 ± 0.14	4.6
7	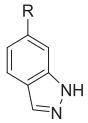	7.77 ± 0.09	6.6	**14**		6.19 ± 0.15	6.2
8	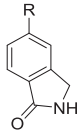	7.74 ± 0.11	7.0	**15**	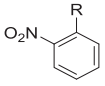	8.07 ± 0.07	6.6
9	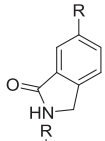	7.32 ± 0.12	6.6	**16**	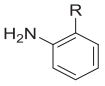	7.57 ± 0.18	6.6
10	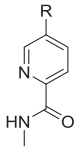	7.86 ± 0.10	7.6				

Entry		pIC$_{50}$ ± SEM	LipE
17	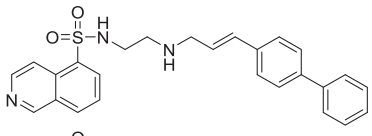	< 5	n.a.
18	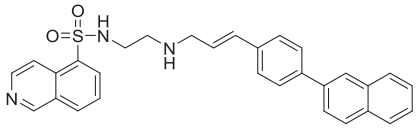	< 5	n.a.

lipE of 7.6. Surprisingly, the nitrogen atom, which plays an important role in the hinge binding to other kinases, was not required for activity. Compounds **13** and **14** retained activity with a pIC$_{50}$ of 7.21 ± 0.34 and 6.19 ± 0.15, respectively. The same was true for the nitro and amino phenyl derivatives **15** and **16**. All together, these results suggested that the binding orientation of the isoquinolinesulfonamides might be different than the one of H-89 in PKA. It was envisioned that the nitrogen atom of the pyridyl ring could act as a potential H-bond acceptor to interact with the hinge region, which may potentially explain the activity of compounds **13–16**. To test this hypothesis compounds (**17–18**), in which the pyridine ring was substituted for a carbacycle, were synthesized (SI Scheme 1). The pIC$_{50}$ of these novel derivatives dropped to < 5 (Table 1). This suggested that the nitrogen in the pyridine is indeed important for the interaction with FLT3 and the isoquinolinesulfonamide may have a flipped binding orientation in the ATP-pocket of FLT3 compared to PKA.[33]

To further understand the SAR of our chemical series, the importance of the linker between the isoquinoline and the pyridyl moieties was investigated (**19–31**). The results from this study are summarized in Table 2. The synthetic schemes for these compounds (**19–31**) are shown in the SI (SI Schemes 1–4). Several analogs were made to investigate possible hydrogen bond donor capability of the sulfonamide and secondary amine group. To this end, the nitrogens of sulfonamide (**19**), amine (**20**) or both (**21**) were substituted with a methyl group. This led to a > 10-fold drop in potency for all compounds, which indicated that these NH donors could be important for

Table 2
FLT3 activity and LipE of compounds **19 – 31**.

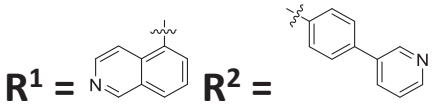

Entry		pIC_{50} ± SEM	LipE
19	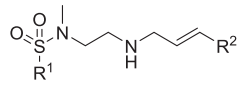	6.74 ± 0.26	5.0
20	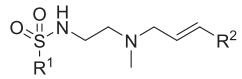	6.87 ± 0.20	4.6
21	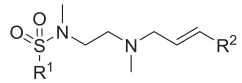	6.90 ± 0.19	4.3
22	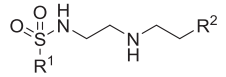	6.57 ± 0.21	5.4
23	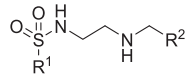	6.80 ± 0.17	5.6
24	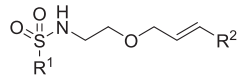	8.08 ± 0.09	5.3
25	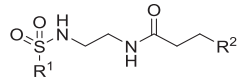	7.49 ± 0.14	5.3
26	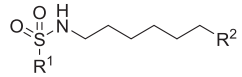	6.77 ± 0.17	2.2
27	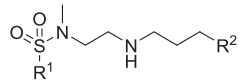	7.32 ± 0.15	5.5
28	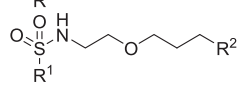	7.41 ± 0.13	4.3
29	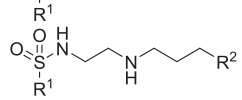	8.05 ± 0.07	6.4
30	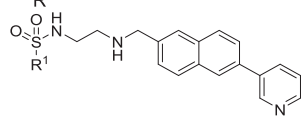	6.25 ± 0.21	3.7
31	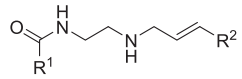	< 5	n.a.

the interaction with FLT3. Next, the linker length between the secondary amine and the phenyl was investigated. Compounds with reduced length of one (**22**) and two (**23**) methylene groups showed decreased activity. The importance of the basicity of the linker moiety was tested by replacing the amine with an ether (**24**), amide (**25**), or a methylene (**26**) containing linker. **24** and **25** were equally active as the corresponding amine derivative, while **26** was > 10-fold less active (Table 2). These results suggested that the basic center of the linker is not required. Of note, reduction of the double bond (**27**–**29**) in the linker resulted in an almost identical inhibitory activity as the parent compound, whereas increasing the conformational restriction in compound **30** reduced its activity. This indicated that the reduced conformational flexibility by the double bond in compound **1** is not beneficial for its activity as has recently been noted for other kinase inhibitors.[34] Finally, the substitution of the sulfonamide for an amide did result in an inactive compound (**31**) (pIC_{50} < 5), which could possibly be due to a difference in the spatial orientation of the (sulfon) amide substituents. These data indicate that a flexible linker of 6 atoms with or without a basic amine is optimal between the sulfonamide and phenyl-pyridyl rings.

Having established the optimal linker features, an additional array of compounds (**32–37**) was synthesized in which the pyridyl ring was replaced with other (substituted) heteroaryls to optimize the hinge-binding interaction (Scheme 2). In contrast to the isoquinoline replacements, a wide range of activities was observed (pIC_{50}: 5 – 8.9) (Table 3). While the picolinamide variations (**34–35**) were inactive (pIC_{50} < 5), the azaindoles **36** and **37** demonstrated a significantly increased pIC_{50} of 8.87 ± 0.06. and 8.78 ± 0.05, respectively. Of note, **37** demonstrated a LipE of 6.7. All together, the optimization of the potential hinge-binding pyridyl moiety resulted in the discovery of the azaindoles as a potent FLT3 inhibitor scaffold.

Next, a matched-molecular pair analysis was performed using the azaindole scaffold with amide (**38–49**) and amine linker (**50–54**) series.[35] The goal was to study the influence of the substitution pattern of the phenyl ring.[36] Compounds (**38–54**) were prepared as shown in Scheme 2. Compounds with electron-withdrawing groups, such as Cl (**39**), *p*-NO_2 (**43**), *p*-F (**45**), or electron donating groups (*p*-Me (**41**) and *p*-OMe (**42**)) both displayed high potency (pIC_{50} > 8.0) (Table 4). No correlation could be found between the Hammett constants of the substituents and the activity of the compounds (SI Figure 1). In fact, non-substituted compound **38** was the most potent compound identified in this study with a pIC_{50} of 9.49 ± 0.08. The matched-molecular pair analysis of LipE values of the amine and amide series showed good correlation, which supports the hypothesis that both series bind in a similar fashion to FLT3 (Figure 2).

Finally, to explain our structure-activity relationships a structure based study was performed with compound **1** and compound **38** using a published DFG-out crystal structure (4RT7), and a DFG-in model (SI Figure 2). Induced fit docking was performed in combination with a previously established binding pose metadynamics protocol[45], in order to determine a feasible binding mode. On the basis of these results and overlap in binding mode with quizartinib (SI Figure 2) it was established that compound **1** and compound **38** bind DFG-out (Figure 3A). The pyridine moiety of **1** is engaged in a hydrogen bond interaction with the backbone of C694 (hinge) and the adjacent phenyl engages in a π-interaction with F691 (Figure 3A). Moreover, in the induced fit experiments no poses were observed in which the isoquinoline interacted with the hinge of FLT3. As shown in Figure 3B the resulting docking pose of **38** is similar to the binding mode of **1** with an additional hydrogen-bond-interaction to C694, which may explain the increased potency. To conclude, the observed binding mode is in agreement with the obtained structure-activity relations.

3. Conclusion

In this study, azaindole **38** was identified as a new, highly potent inhibitor of FLT3-ITD with favorable physico-chemical properties. Our structure-activity relationships and modeling studies suggest that **38** has an alternative flipped binding mode compared to other kinase inhibitors derived from the prototypical kinase inhibitor H-89. **38** forms an excellent starting point for further lead optimization studies to obtain clinical candidates to modulate FLT3-ITD in AML patients.

4. Experimental

4.1. Chemistry

All of the compounds were synthesized as shown in Schemes 1–2 and Supplementary Schemes 1–5. Detailed procedures and characterization data are described in the Supplementary Information.

4.2. Biochemical evaluation of FLT3 inhibitors

In a 384-wells plate (PerkinElmer 384 Flat White), 5 µL kinase/

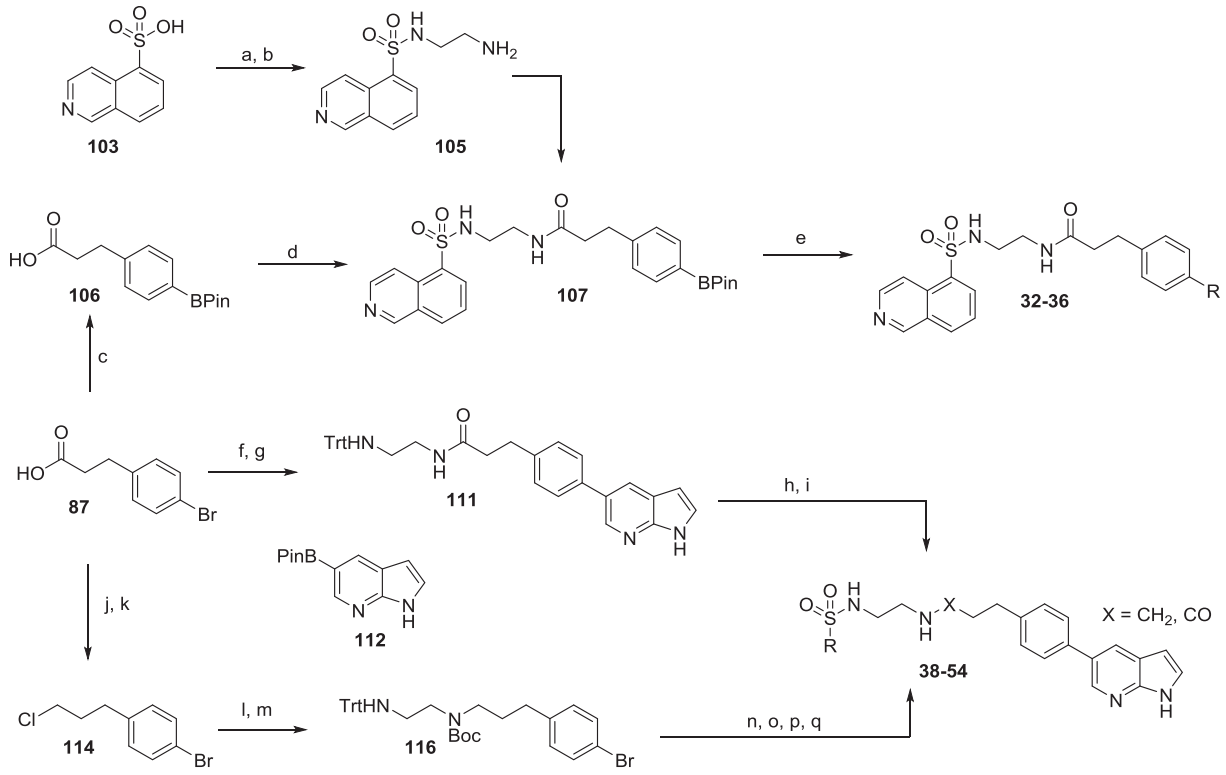

Scheme 2. Synthetic route towards the derivatives **32–36** and **38–54**.[a] [a]Reagents and conditions: (a) $SOCl_2$, DMF, reflux, 4 h; (b) ethylenediamine, DCM, 0 °C – RT; (c) B_2Pin_2, KOAc, $Pd(dppf)Cl_2$, 1,4-dioxane, 100 °C, overnight; (d) **105**, EDC, HOBt, DiPEA, DCM, 4 h; (e) heteroaryl-bromide, $Pd(PPh_3)_4$, K_2CO_3, DMF, 85 °C, overnight; (f) **60**, EDC, HOBt, DiPEA, DCM, 4 h; (g) **112**, $Pd(PPh_3)_4$, K_2CO_3, DMF, 90 °C; (h) TFA, TES, DCM, 0 °C – RT, 16 h; (i) aryl-sulfonylchloride, Et_3N, DCM/DMF, 0 °C – RT, 16 h; (j) $NaBH_4$, BF_3, THF, 0° - RT, 16 h; (k) $SOCl_2$, DMF, 0 °C – RT, 19 h; (l) **60**, K_2CO_3, ACN, 70 °C, 72 h; (m) $NaHCO_3$, Boc_2O, THF, RT, 36 h; (n) **112**, $Pd(PPh_3)_4$, K_2CO_3, DMF, 90 °C; (o) TFA, TES, DCM, 0 °C – RT, 20 h; (p) aryl-sulfonylchloride, Et_3N, DCM/DMF, 0 °C – 30 °C, 16 h (q) TFA, DCM, 0 °C – RT, 16 h.

Table 3
FLT3 activity and LipE of compounds **32–37**.

R =

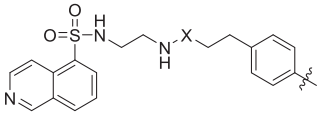

Entry		X	pIC_{50} ± SEM	LipE
32		CO	6.82 ± 0.14	4.8
33	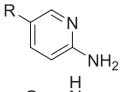	CO	7.63 ± 0.11	5.6
34	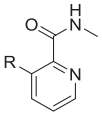	CO	< 5	n.a.
35	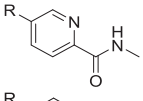	CO	< 5	n.a.
36	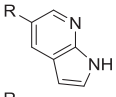	CO	8.87 ± 0.06	6.2
37	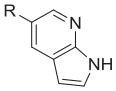	CH_2	8.78 ± 0.05	6.7

peptide mix (0.06 ng/µL FLT3 (Life Technologies; PV3182; Lot: 1614759F), 200 nM peptide (PerkinElmer; Lance® Ultra ULightTM TK-peptide; TRFO127-M; Lot: 2178856)) in assay buffer (50 mM HEPES pH 7.5, 1 mM EGTA, 10 mM $MgCl_2$, 0.01% Tween-20, 2 mM DTT) was dispensed. Separately inhibitor solutions (10 µM – 0.1 pM) were prepared in assay buffer containing 400 µM ATP and 1% DMSO. 5 µL of these solutions were dispensed and the plate was incubated in the dark at room temperature. After 90 min the reaction was quenched by the addition of 10 µL of 20 mM EDTA containing 4 nM antibody (PerkinElmer; Lance® Eu-W1024-anti-phosphotyrosine (PT66); AD0068; Lot: 2342358). After mixing, samples were incubated for 60 min in the dark. The FRET fluorescence was measured on a Tecan Infinite M1000 Pro plate reader (excitation 320 nm, emission donor 615 nm, emission acceptor 665 nm). Data was processed using Microsoft Excel 2016, pIC_{50} values were fitted using GraphPad Prism 7.0. Final assay concentrations during reaction: 200 µM ATP, 0.03 ng/µL FLT3, 100 nM Lance TK-peptide, 0.5% DMSO. Compounds were tested in n = 2 and N = 2.

4.3. Structure based modeling on FLT3

All structure based modeling was performed in the Schrödinger suite (Schrödinger Release 2017-4: Maestro, Schrödinger, LLC, New York, NY, 2017). Crystal structures were prepared using the protein preparation wizard,[37] ligands were prepared using LigPrep.[38] Both the DFG-out structure co-crystalized with quizartinib (4RT7)[39] and a DFG-in model were used in order to dock our initial compound **1**. The DFG-in model was constructed on the basis of 4RT7 and 3LCD, in a similar fashion as has been done before,[40] using the knowledge based potential in prime.[41,42] Docking was done using induced fit docking and using H-bond constraints on C694.[43] In order to determine to correct binding pose, induced fit

Table 4
FLT3 activity and LipE of compounds **38–54.**

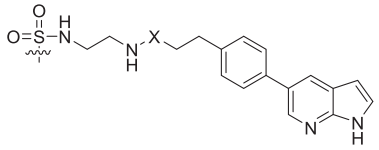

Entry		X	pIC_{50} ± SEM	LipE
38		CO	9.49 ± 0.08	6.5
39	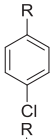	CO	8.62 ± 0.05	5.0
40	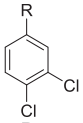	CO	8.39 ± 0.05	4.1
41	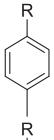	CO	8.67 ± 0.06	5.2
42	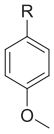	CO	8.74 ± 0.08	5.8
43	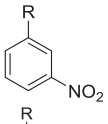	CO	8.80 ± 0.08	5.9
44		CO	8.72 ± 0.06	5.1
45	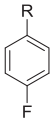	CO	9.39 ± 0.18	6.2
46	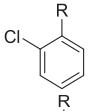	CO	9.32 ± 0.09	5.7
47	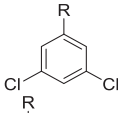	CO	8.16 ± 0.08	3.9
48	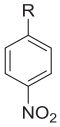	CO	7.97 ± 0.09	5.0
49	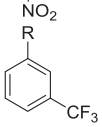	CO	8.37 ± 0.09	4.5
50		CH_2	8.88 ± 0.06	6.5
51	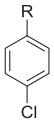	CH_2	8.36 ± 0.08	6.4

Table 4 (*continued*)

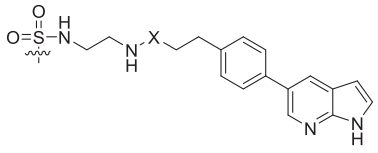

Entry		X	pIC_{50} ± SEM	LipE
52	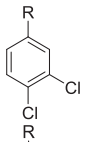	CH_2	8.13 ± 0.09	4.5
53	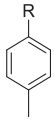	CH_2	8.69 ± 0.07	5.9
54	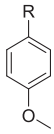	CH_2	8.62 ± 0.10	6.3

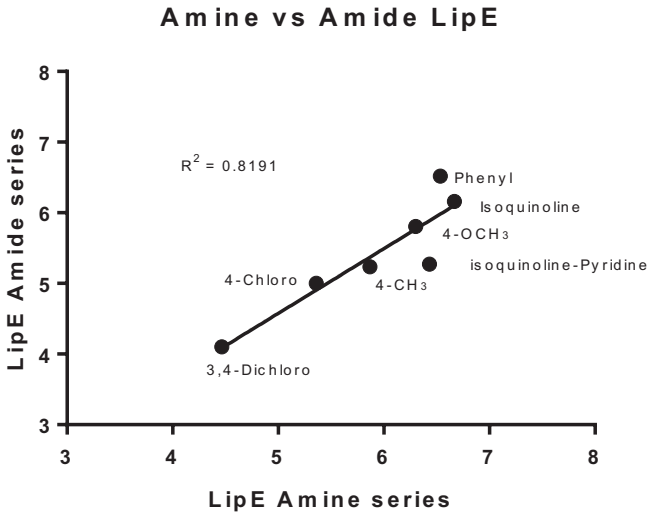

Figure 2. Matched molecular pair analysis of amine and amide containing compounds. Data shows a high correlation (R^2 = 0.82), indicating a similar binding mode for both linker series.

docking was followed by the conformer cluster script, using the Kelley criterion[44] to determine the optimal number of clusters. The highest scoring poses of every cluster were used in a previously published workflow to determine binding poses[45], which is based on metadynamics. The highest scoring pose was selected by adding the Metadynamics CompScore to the docking score. Based on this workflow the highest scoring pose was visualized and rendered using PyMol.[46]

Acknowledgements

None.

Contributions

Cancer Drug Discovery Initiative (CDDI) is acknowledged for funding. SG, BG, JK, NL and RW performed the organic synthesis and

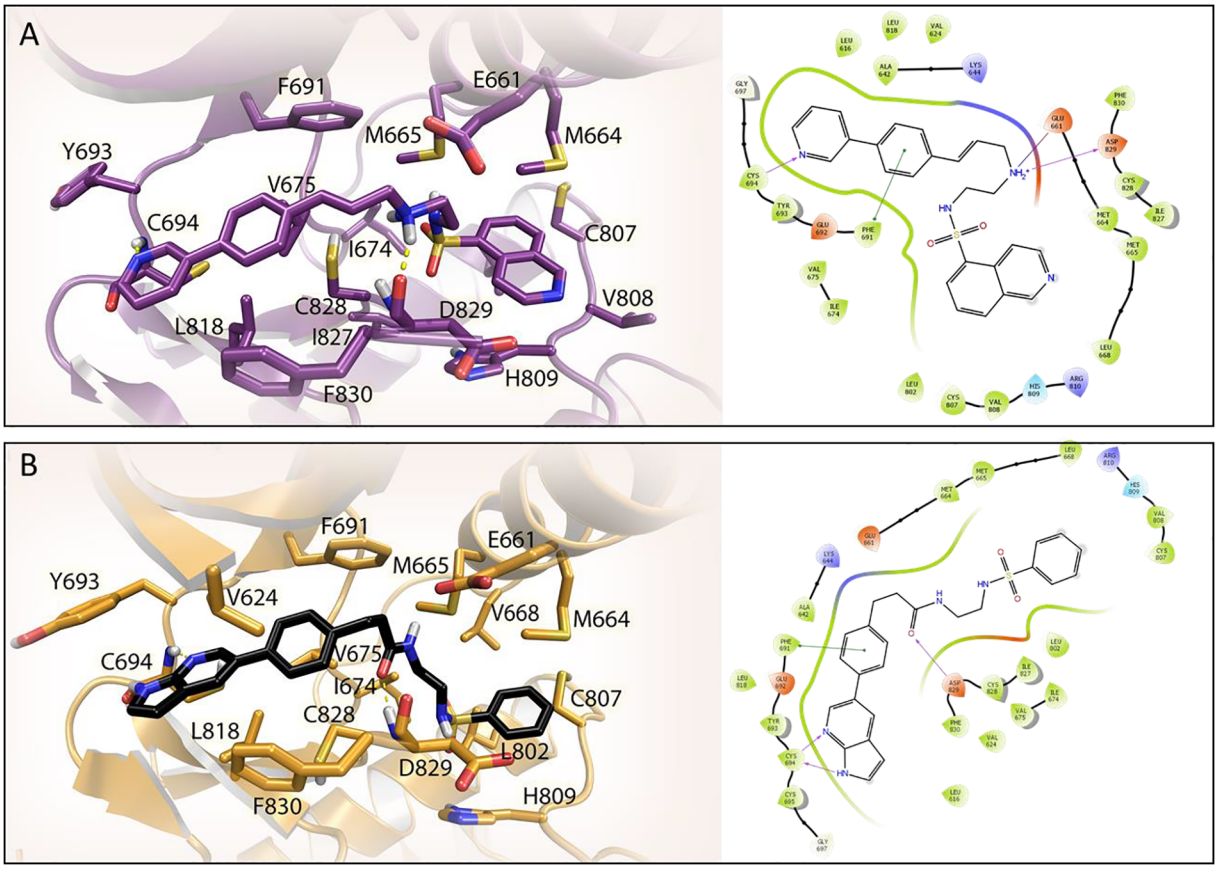

Figure 3. Proposed "flipped" binding mode of **1** and **38** in FLT3. (A-left) **1** and (B-left) **38** docked in FLT3 crystal structure (PDB: 4RT7). On the right a 2D-interaction diagram is shown depicting the interactions between the ligand and FLT3.

biochemical evaluation. EL and GW performed the docking studies and provided LogD calculations. SG, RW, CB, HO, JN and MS designed the experiments. SG and MS wrote the manuscript.

Competing interests

Declarations of interest: none.

Appendix A. Supplementary data

Supplementary data to this article can be found online at https://doi.org/10.1016/j.bmc.2019.01.006.

References

1. Shipley JL, Butera JN. Acute Myelogenous Leukemia. *Exp Hematol.* 2009;37(6):649–658.
2. Döhner H, Weisdorf DJ, Bloomfield CD. Acute Myeloid Leukemia. *N Engl J Med.* 2015;373(12):1136–1152.
3. Döhner H, Estey EH, Amadori S, et al. Diagnosis and Management of Acute Myeloid Leukemia in Adults: recommendations from an International Expert Panel, on Behalf of the European LeukemiaNet. *Blood.* 2010;115(3):453–474.
4. Fathi AT, Chen Y-B. The Role of FLT3 Inhibitors in the Treatment of FLT3-Mutated Acute Myeloid Leukemia. *Eur J Haematol.* 2017;98(4):330–336.
5. Stirewalt DL, Radich JP. The Role of FLT3 in Haematopoietic Malignancies. *Nat Rev Cancer.* 2003;3(9):650–665.
6. Leung AYH, Man C-H, Kwong Y-L. FLT3 Inhibition: A Moving and Evolving Target in Acute Myeloid Leukaemia. *Leukemia.* 2012;27(2):260–268.
7. Pemmaraju N, Kantarjian H, Ravandi F, Cortes J. FLT3 Inhibitors in the Treatment of Acute Myeloid Leukemia: The Start of an Era? *Cancer.* 2011;117(15):3293–3304.
8. Kayser S, Levis MJ. Advances in Targeted Therapy for Acute Myeloid Leukaemia. *Br J Haematol.* 2018;180(4):484–500.
9. Levis M. Midostaurin Approved for FLT3-Mutated AML. *Blood.* 2017;129(26):3403–3406.
10. Zimmerman EI, Turner DC, Buaboonnam J, et al. Crenolanib Is Active against Models of Drug-Resistant FLT3-ITD-Positive Acute Myeloid Leukemia. *Blood.* 2013;122(22):3607–3615.
11. Baker SD, Zimmerman EI, Wang Y-D, et al. Emergence of Polyclonal FLT3 Tyrosine Kinase Domain Mutations during Sequential Therapy with Sorafenib and Sunitinib in FLT3-ITD-Positive Acute Myeloid Leukemia. *Clin Cancer Res.* 2013;19(20):5758–5768.
12. Smith CC, Wang Q, Chin C-S, et al. Validation of ITD Mutations in FLT3 as a Therapeutic Target in Human Acute Myeloid Leukaemia. *Nature.* 2012;485(7397):260–263.
13. Man CH, Fung TK, Ho C, et al. Sorafenib Treatment of FLT3-ITD(+) Acute Myeloid Leukemia: Favorable Initial Outcome and Mechanisms of Subsequent Nonresponsiveness Associated with the Emergence of a D835 Mutation. *Blood.* 2012;119(22):5133–5143.
14. Smith CC, Lasater Ea, Zhu X, Lin KC, Stewart WK, Damon LE, Salerno S, Shah NP. Activity of Ponatinib against Clinically-Relevant AC220-Resistant Kinase Domain Mutants of FLT3-ITD. *Blood.* 2013;121(16):3165–3171.
15. Liu N. *Development of Kinase Inhibitors and Activity-Based Probes.* Leiden University; 2016.
16. Fedorov O, Marsden B, Pogacic V, et al. A Systematic Interaction Map of Validated Kinase Inhibitors with Ser/Thr Kinases. *Proc. Natl. Acad. Sci. USA.* 2007;104(51):20523–20528.
17. Chijiwa T, Mishima A, Hagiwara M, et al. Inhibition of Forskolin-Induced Neurite Outgrowth and Protein Phosphorylation by a Newly Synthesized Selective Inhibitor of Cyclic AMP-Dependent Protein Kinase, N-[2-(P-Bromocinnamylamino)ethyl]-5-Isoquinolinesulfonamide (H-89), of PC12D Pheochromocytoma Cells. *J Biol Chem.* 1990;265(9):5267–5272.
18. Pflug A, Johnson KA, Engh RA. Anomalous Dispersion Analysis of Inhibitor Flexibility: A Case Study of the Kinase Inhibitor H-89. *Acta Crystallogr Sect F Struct Biol Cryst Commun.* 2012;68(8):873–877.
19. Gao Y, Davies SP, Augustin M, et al. A Broad Activity Screen in Support of a Chemogenomic Map for Kinase Signalling Research and Drug Discovery. *Biochem J.* 2013;451(2):313–328.
20. Lochner A, Moolman JA. The Many Faces of H89: A Review. *Cardiovasc Drug Rev.* 2006;24(3–4):261–274.
21. Kuijl C, Savage NDL, Marsman M, et al. Intracellular Bacterial Growth Is Controlled by a Kinase Network around PKB/AKT1. *Nature.* 2007;450(7170):725–730.
22. Csizmadia F, Tsantili-Kakoulidou A. Panderi I.; Darvas F. Prediction of Distribution Coefficient from Structure. 1. Estimation Method. *J Pharm Sci.* 1997;86(7):865–871.
23. Johnson TW, Gallego RA, Edwards MP. Lipophilic Efficiency as an Important Metric in Drug Design. *J Med Chem.* 2018 acs.jmedchem.8b00077.
24. Wu P, Nielsen TE, Clausen MH. FDA-Approved Small-Molecule Kinase Inhibitors.

Trends Pharmacol Sci. 2015;36(7):422–439.
25. Martin MP, Alam R, Betzi S, Ingles DJ, Zhu J-Y, Schönbrunn E. A Novel Approach to the Discovery of Small-Molecule Ligands of CDK2. *ChemBioChem.* 2012;13(14):2128–2136.
26. Gajiwala KS, Wu JC, Christensen J, et al. KIT Kinase Mutants Show Unique Mechanisms of Drug Resistance to Imatinib and Sunitinib in Gastrointestinal Stromal Tumor Patients. *Proc Natl Acad Sci USA.* 2009;106(5):1542–1547.
27. Hilberg F, Roth GJ, Krssak M, et al. BIBF 1120: Triple Angiokinase Inhibitor with Sustained Receptor Blockade and Good Antitumor Efficacy. *Cancer Res.* 2008;68(12):4774–4782.
28. Awad MM, Katayama R, McTigue M, et al. Acquired Resistance to Crizotinib from a Mutation in CD74 – ROS1. *N Engl J Med.* 2013;368(25):2395–2401.
29. Chen P, Lee NV, Hu W, et al. Spectrum and Degree of CDK Drug Interactions Predicts Clinical Performance. *Mol Cancer Ther.* 2016;15(10):2273–2281.
30. Pemovska T, Johnson E, Kontro M, et al. Axitinib Effectively Inhibits BCR-ABL1(T315I) with a Distinct Binding Conformation. *Nature.* 2015;519(7541):102–105.
31. McTigue M, Murray BW, Chen JH, Deng Y-L, Solowiej J, Kania RS. Molecular Conformations, Interactions, and Properties Associated with Drug Efficiency and Clinical Performance among VEGFR TK Inhibitors. *Proc. Natl. Acad. Sci. USA.* 2012;109(45):18281–18289.
32. Xing L, Rai B, Lunney EA. Scaffold Mining of Kinase Hinge Binders in Crystal Structure Database. *J Comput Aided Mol Des.* 2014;28(1):13–23.
33. Shavnya A, Coffey SB, Smith AC, Mascitti V. Palladium-Catalyzed Sulfination of Aryl and Heteroaryl Halides: Direct Access to Sulfones and Sulfonamides. *Org Lett.* 2013;15(24):6226–6229.
34. Wienen-Schmidt B, Jonker HRA, Wulsdorf T, et al. Flexible Ligand Binds Most Entropy-Favored: Intriguing Impact of Ligand Flexibility and Solvation on Drug-Kinase Binding. *J Med Chem.* 2018 acs.jmedchem.8b00105.
35. Dossetter AG, Griffen EJ, Leach AG. Matched Molecular Pair Analysis in Drug Discovery. *Drug Discov Today.* 2013;18(15–16):724–731.
36. Topliss JG. Utilization of Operational Schemes for Analog Synthesis in Drug Design. *J Med Chem.* 1972;15(10):1006–1011.
37. Schrödinger Release 2017-4: Schrödinger Suite 2017-4 Protein Preparation Wizard; Epik, Schrödinger, LLC, New York, NY, 2017; Impact, Schrödinger, LLC, New York, NY, 2017; Prime, Schrödinger, LLC, New York, NY, 2017.
38. Schrödinger Release 2017-4: LigPrep, Schrödinger, LLC, New York, NY, 2018.
39. Smith CC, Zhang C, Lin KC, et al. Characterizing and overriding the structural mechanism of the quizartinib-resistant FLT3 “gatekeeper” F691L mutation with PLX3397. *Cancer Discov.* 2015;5:668–679.
40. Ke Y-Y, Singh VK, Coumar MS, et al. Homology modeling of DFG-in FMS-like tyrosine kinase 3 (FLT3) and structure-based virtual screening for inhibitor identification. *Sci Rep.* 2015;5:11702.
41. Jacobson MP, Pincus DL, Rapp CS, et al. A hierarchical approach to all-atom protein loop prediction. *Proteins Struct Funct Bioinf.* 2004;55:351–367.
42. Jacobson MP, Friesner RA, Xiang Z, Honig B. On the role of the crystal environment in determining protein side-chain conformations. *J Mol Biol.* 2002;320:597–608.
43. Sherman W, Day T, Jacobson MP, Friesner RA, Farid R. Novel procedure for modeling ligand/receptor induced fit effects. *J MedChem.* 2006;49:534–553.
44. Kelley LA, Gardner SP, Sutcliffe MJ. An automated approach for clustering an ensemble of NMR-derived protein structures into conformationally related subfamilies. *Protein Eng Des Sel.* 1996;9:1063–1065.
45. Clark AJ, Tiwary P, et al. Prediction of protein–ligand binding poses via a combination of induced fit docking and metadynamics simulations. *J Chem Theory Comput.* 2016;12:2990–2998.
46. The PyMOL Molecular Graphics System, Version 1.8 Schrödinger, LLC.